NUMERICAL SIMULATION OF AIRFLOW AROUND VEHICLE MODELS

Nguyen Van Thang[1, *], Ha Tien Vinh[1], Bui Dinh Tri[1, 2], Nguyen Duy Trong[1]

[1]*Institute of Mechanics, Vietnam Academy of Science and Technology*
[2]*Vietnam Academy of Science and Technology*

[*]Email*: thangnv2010@gmail.com*

Abstract. This article carries out the numerical simulation of airflow over three dimensional car models using ANSYS Fluent software. The calculations have been performed by using realizable k-ɛ turbulence model. The external airflow field of the simplified BMW M6 model with or without a wing is simulated. Several aerodynamic characteristics such as pressure distribution, velocity contours, velocity vectors, streamlines, turbulence kinetic energy and turbulence dissipation energy are analyzed in this study. The aerodynamic forces acting on the car model is calculated and compared with other authors. A rear wing shows a slight increase in the drag coefficient and a remarkable decrease in the lift coefficient. A change of lift force thus improves the car stability.

Key words: k-ɛ turbulence model, automotive aerodynamics, drag, lift

Classification numbers: 5.4.4; 5.6.2; 5.10.2.

1. INTRODUCTION

In recent decades, computational fluid dynamics (CFD) has been playing an important role in engineering and industrial problems. The CFD technology has applied in research, design and improvement of aerodynamic car geometry. Therefore, automotive industry has a rapid development every year.

The Ahmed model was described and performed experimentally by Admed et al. [1]. Two test cases with slant angles of 25 and 35 degrees are estimated. The drag force caused by air flow over the car body at velocities of 40 and 60 m/s is examined. Aljure et al. [2] carried out the numerical simulations of flow around two car models, the Ahmed and the Asmo cars to investigate turbulent structures. The unsteady turbulent characteristics such as velocity profile, pressure distribution, vortex shedding, flow reattachment and recirculation bubbles around car bodies are estimated. The lift and drag coefficients are also calculated. The numerical results are compared with experiments. Brunn et al. [3] performed experimental and numerical investigations in order to reduce the total aerodynamic drag of the Ahmed car model at the slant angles of 25 and 35 degrees. Both experimental and numerical results showed a weakening of a

span-wise vortex in the separated flow past the slant edge which is strongly coupled with the occurrence of stronger streamwise vortices along the slant edges and vice versa.

In order to consider the change of lift and drag forces acting on a car model when a rear spoiler is attached, Hu and Wong [4] carried out numerical simulations of air flow over the simplified Camry model with or without a rear spoiler using the standard k-ε model. Computational results indicate that the designed rear spoiler reduce inconsiderably the drag force and increase the lift force. In 2012, Kodali and Bezavada [5] performed numerical simulations of airflow over a passenger car with or without a rear spoiler using CFD. The obtained results of aerodynamic forces represent that the presence of rear spoiler reduces around 80 % in the lift coefficient and increases around 3 % in the drag coefficient. In addition, there is 48 % decrease in the minimum static pressure and 14 % increase in the maximum static pressure on the car's surface due to the attachment of a rear spoiler.

In the present paper, we address numerical investigations of airflow over two three-dimensional car models, the Ahmed and BMW M6 cars. The commercial ANSYS Fluent software is employed. The realizable k-ε turbulence model is used to compute at the air velocity of 40 m/s. The turbulent flow structures are obtained and estimated. In addition, the drag coefficient is calculated to consider the force acting on the Ahmed car and compared with other numerical and experimental simulations.

2. NUMERICAL APPROACH

Figure 1 illustrates the dimensions and 3D shape of Ahmed car. This model is created by Ahmed [1] and then it has been used in several numerical and experimental works. In our study, the 3D Ahmed model with the rear slant angle of 25 degrees is employed to validate the model. The air velocity at inlet is 40 m/s. The mesh used for this case is also depicted in Figure 1. Total element number is about 2.9 million. The simplified BMW M6 models without and with a rear wing are indicated in Figure 2. The dimensions of the BMW M6 model car is 5.011 m x 2.106 m x 1.395 m. Tetrahedral mesh type is used with about 3.0 million elements. The speed of vehicle used for numerical simulations is 40 m/s. The realizable k-ε turbulence model is employed for all numerical calculations.

The realizable k-ε turbulence equations for incompressible flow have forms as following:

For turbulent kinetic energy k

$$\frac{\partial}{\partial t}\left(\rho k\right) + \frac{\partial}{\partial x_i}\left(\rho k u_j\right) = \frac{\partial}{\partial x_j}\left[\left(\mu + \frac{\mu_t}{\sigma_k}\right)\frac{\partial k}{\partial x_j}\right] + 2\mu_t S_{ij}S_{ij} - \rho\varepsilon \tag{1}$$

For dissipation ε

$$\frac{\partial}{\partial t}\left(\rho\varepsilon\right) + \frac{\partial}{\partial x_j}\left(\rho\varepsilon u_j\right) = \frac{\partial}{\partial x_j}\left[\left(\mu + \frac{\mu_t}{\sigma_\varepsilon}\right)\frac{\partial\varepsilon}{\partial x_j}\right] + C_{1\varepsilon}\frac{\varepsilon}{k}2\mu_t S_{ij}S_{ij} - \rho C_{2\varepsilon}\frac{\varepsilon^2}{k + \overline{v\varepsilon}} \tag{2}$$

where, the eddy viscosity is obtained

$$\mu_t = \rho C_\mu \frac{k^2}{\varepsilon} \tag{3}$$

and the strain tensor is defined as

$$S_{ij} = \frac{1}{2}\left(\frac{\partial u_j}{\partial x_i} + \frac{\partial u_i}{\partial x_j}\right) \tag{4}$$

$C_{1\varepsilon}, C_{2\varepsilon}, \sigma_k$ và σ_ε are constant.

$$C_\mu = 0.09, C_{1\varepsilon} = 1.44, C_{2\varepsilon} = 1.9, \sigma_k = 1.0, \sigma_\varepsilon = 1.2$$

In our simulation, a rectangular domain is used. The inlet boundary is set velocity inlet. The outlet boundary is pressure outlet. The side and top walls is no-slip. The ground (bottom wall) is also no-slip. In our simulations, in order to examine aerodynamic forces, drag and lift coefficients are calculated. Drag and lift coefficients are defined as following equations:

$$C_D = \frac{F_D}{\frac{1}{2}\rho U^2 A} \tag{5}$$

$$C_L = \frac{F_L}{\frac{1}{2}\rho U^2 A} \tag{6}$$

where F_D and F_L are the drag and lift forces, respectively, U is the vehicle speed, ρ is the air density, and A is the frontal projected area of the vehicle. For the Ahmed model, the value of A is 0.112 m^2 and for the BMW M6 model, this value is set 1.1 m^2, corresponding of vehicle geometry. Pressure coefficient is also calculated in this work. This coefficient is defined as follows:

$$C_p = \frac{p - p_\infty}{\frac{1}{2}\rho U^2} \tag{7}$$

where C_p is the pressure coefficient, p_∞ is the infinite pressure.
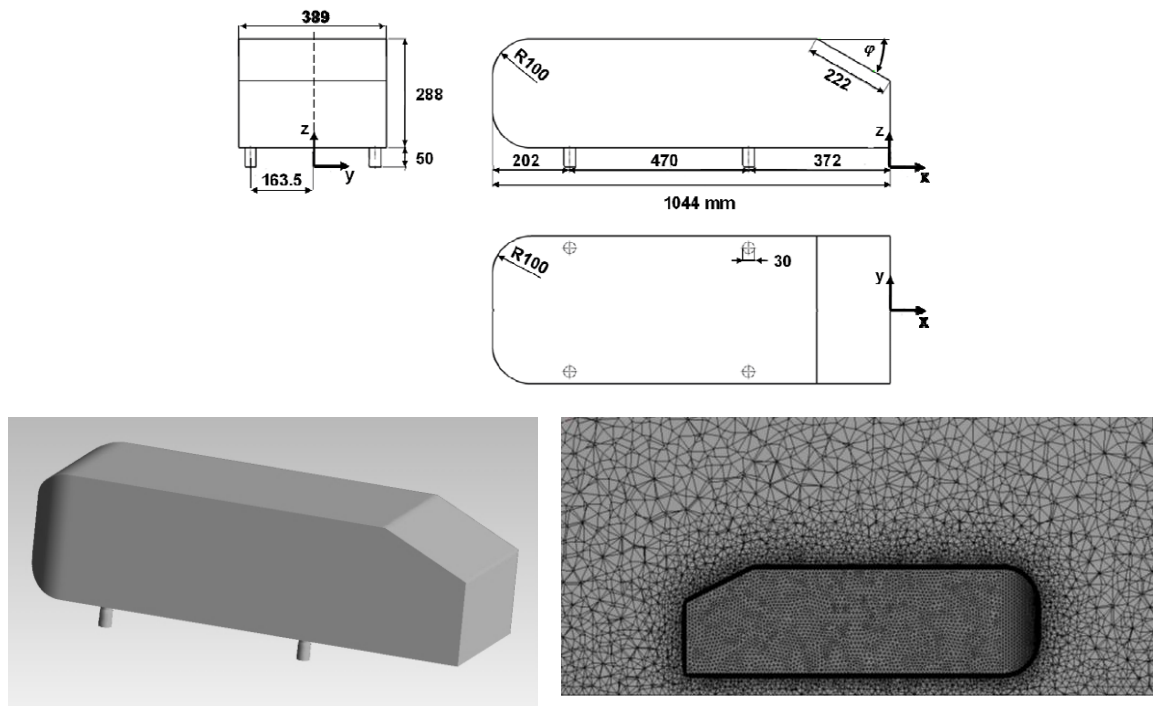

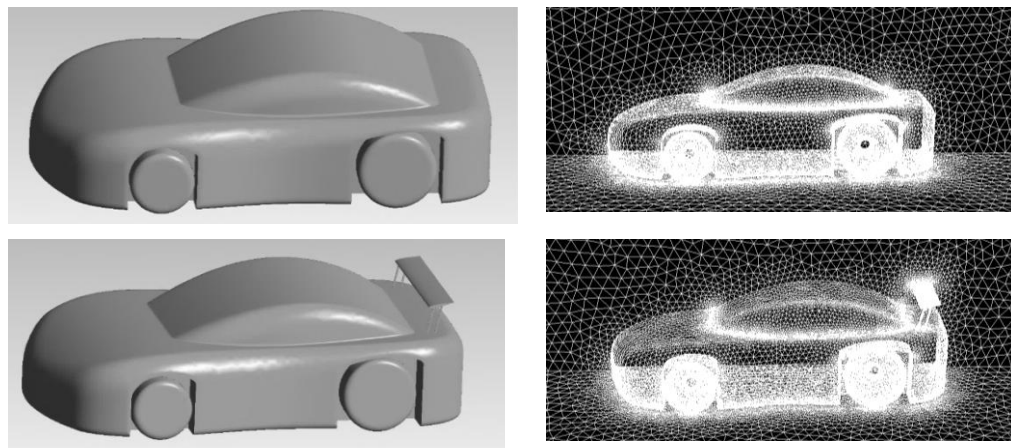*Figure 1*. Ahmed model: Dimensions, 3D model and the mesh

Figure 2. BMW M6 model without/with a wing and grid distribution near the car body

3. RESULTS AND DISCUSSIONS

3.1. Airflow over the Ahmed model

Table 1. Ahmed car drag coefficient (C_L) with different numerical and experimental results

	Drag coefficient	Error (%)
Ahmed [1]	0.285	--
Aljure et al (VMS) [2]	0.292	2.46
Brunn et al (exp) [3]	0.41	43.86
Meile et al (exp) [6]	0.299	4.91
Meile et al (Fluent) [6]	0.295	3.51
Guilmineau (SST k-ω) [7]	0.307	7.72
Kapadia et al (RANS) [8]	0.3272	14.81
Parab et al(Realizable k-ε) [9]	0.291	2.11
Present study	0.293	2.81

The Ahmed body with a rear slant angle of 25° is employed. Simulation results are compared with other numerical and experimental calculations. Table 1 illustrates a comparison of the drag coefficient between our computation and various simulations and experiments [2-3, 6-9] including Ahmed's result [1], drag coefficient is 0.285. The error values in the table are obtained by estimating a difference between Ahmed's drag coefficient and others' ones. The comparison indicates that our computation of drag coefficient is close to Ahmed's result with the error value of 2.81 %. The maximum error value is appeared in experimental investigation by Brunn et al [2], 43.86 %, whereas the minimum error can be seen in the calculation of Parab et al. [9], 2.11 %. The distribution of pressure coefficient contours is illustrated in Figure 3. The high pressure bubbles around the Ahmed car can be seen. The wider bubble appeared in the front of car. And the smaller bubbles appeared on the curved edges of the car's head and at the corner on

the upper surface of the car. Figure 4 shows the recirculation behind the car body. Obviously, there are two vortices generated by the air flow coming down the slant rear back of the body and the flow from the under body. The recirculation of the upper vortex is larger than that of the lower vortex. However, they have the same length.
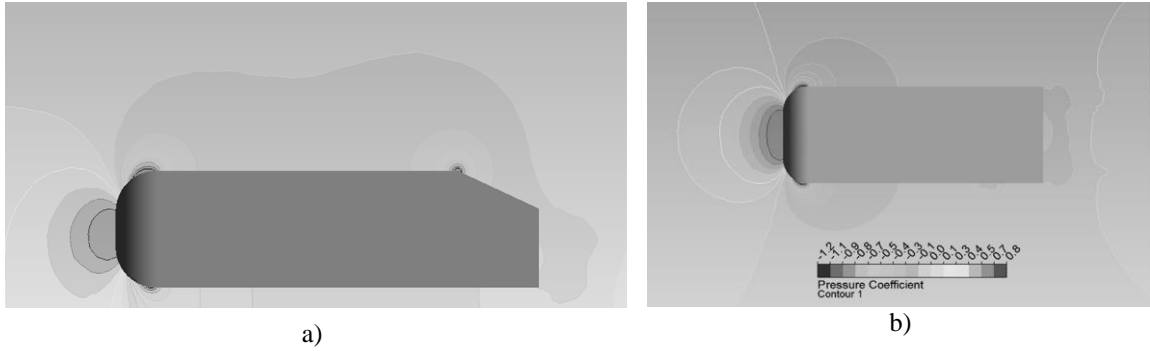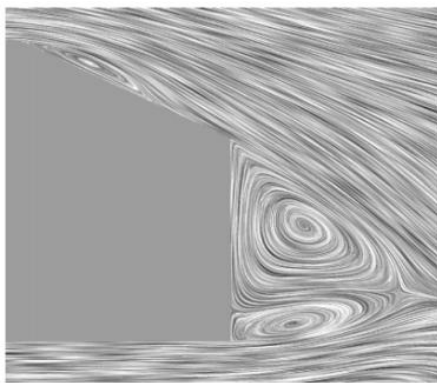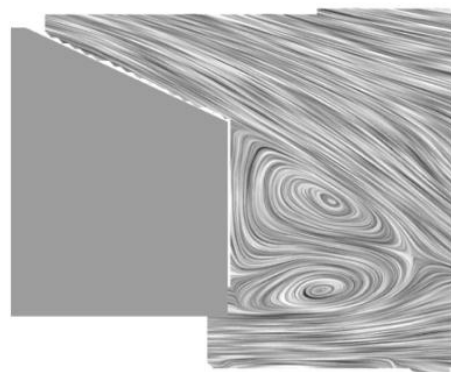

a)

b)

Figure 3. Distribution of pressure coefficient contours: This study (left column); and (b) Aljure et al. (right column)

(a) Present study

(b) Brunn et al. (LES) [3]

(c) Brunn et al. (Exp.) [3]

Figure 4. Recirculation behind the car body

Figure 5 indicates the counter-rotating trailing vortex system near the car on the vertical planes which have the distance from the back of the car is 0 mm, 80 mm, and 200 mm. The simulated results are compared with the work of Lienhart et al. [10]. On the 0 mm and 80 mm planes, there are two separated small trailing vortices on the top edge, while on the 200 mm plane these vortices are closer but larger than that at two previous plans. On three planes, the air flow intends going from the top to the bottom. The velocity magnitude increases when the plane is further.
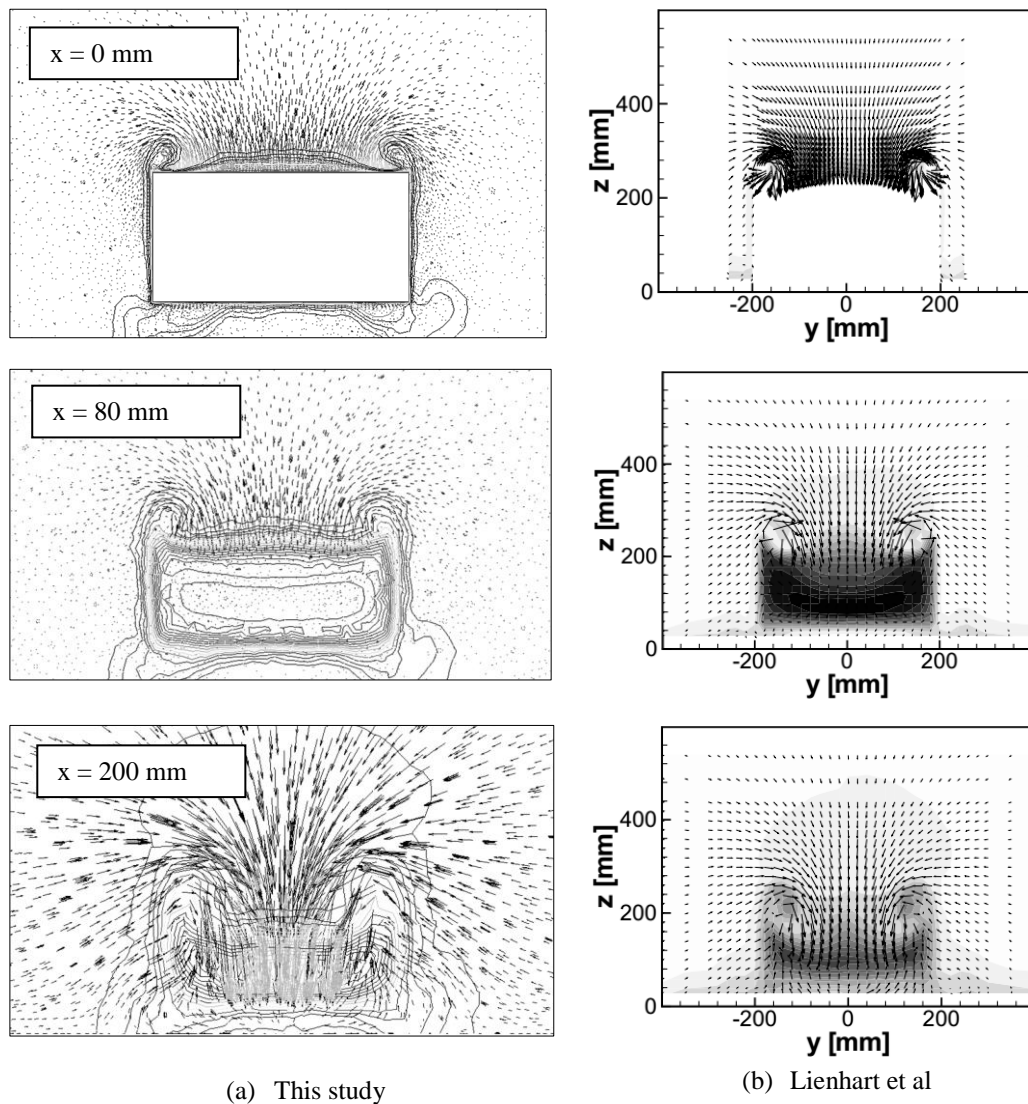

(a) This study

(b) Lienhart et al

Figure 5. Illustration of the counter-rotating trailing vortex system.

3.2. Airflow over the BMW M6 model

The importance of two aerodynamic parameters, drag and lift forces are mentioned in Aljure et al. [2]. Study on reduction of the drag coefficient acting on the vehicle has been attractive to many experimental and numerical investigations. That reducing of the drag

coefficient will reduce fuel consumption. Whereas, reducing the lift coefficient will increase the stability and cornering performance of a vehicle. Table 2 shows the calculated drag coefficient of air flow acting on the BMW M6 model. The value obtained in this study is 0.377, while the drag coefficient (technical specification) of real car is 0.39 [11]. To investigate the effect of wing on drag and lift coefficients acting on the model, these values can be seen in Table 3 when the speed is 40 m/s, about 150 km/h. It found that the wing makes the drag coefficient increased 5.28 % and makes the lift coefficient decreased 31.25 %. It means the rear wing improves car's riding stability and cornering performance. This is very important if a vehicle is travelling at a very high speed, especially a F1 racing car. Contours of pressure distribution around the car model without/with a wing can be observed in Figure 6. It is able to see that high pressure appears in front of car, and low pressure on the top of car. As mentioned in Table 3, the drag force has 5.28 % difference between the original (without a wing) and modified (with a wing) models because pressure distributions in front of car and on the top of car are almost same. Pressure distribution at upper part of car is obviously different between two car models, especially, at the rear part where the wing is attached. This causes drag force's value of the modified model is smaller than that of the original model.

Figure 7 illustrates the contours of velocity distribution around BMW M6 model without a wing (Fig. 7a) and with a wing (Fig. 7b). Since there is a wing attached at the rear back of the car, the velocity distribution behind the model with a wing is remarkably different in comparing with which behind the model without a wing. The velocity distribution has formed a long tail from the car back.

Table 2. Comparison of the drag coefficient between this study and real BMW M6

	Drag coefficient	Error (%)
BMW M6 [10]	0.39	-
Present study	0.377	3.33

The turbulence kinetic energy (TKE) distribution around BMW M6 model without and with a wing is indicated in Figure 8. The TKE is characterized by fluid shear, friction or complex shape of an object that external flow is over. Generally, the TKE is estimate by the mean of the turbulence normal stresses $k = \frac{1}{2}u'_{\iota}u'_{\iota}$ or obtained from the turbulence equations (1) and (2). It is obvious that the area of the high TKE distribution behind the car with a wing (Fig. 8b) is larger than that behind the car without a wing (Fig. 8a). It means the rear wing causes strong turbulence of air flow behind the car. Additionally, the TKE distribution is concentrated behind the model with a wing.

Table 3. Drag and lift coefficient acting on the BMW M6 model with/without a rear wing

	Drag coefficient	Lift coefficient
Without a wing	0.377	-0.173
With a wing	0.397	-0.227
Error (%)	5.28	31.25

(a) BMW M6model

(b) BMW M6 model with a wing
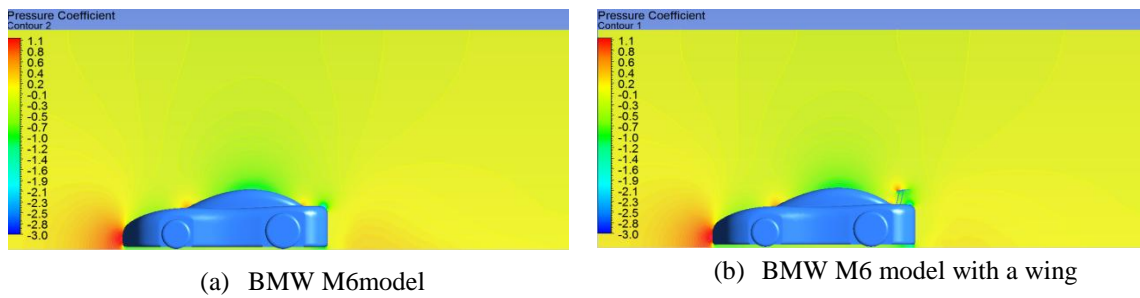
Figure 6. Contours of pressure distribution around BMW M6 model without/with a wing

(a) BMW M6 model

(b) BMW M6 model with wing
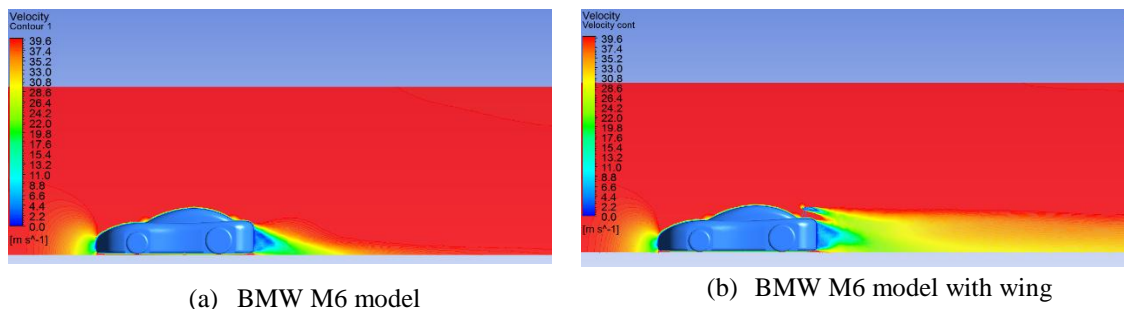
Figure 7. Contours of velocity distribution around BMW M6 model without/with a wing

(a) BMW M6 model
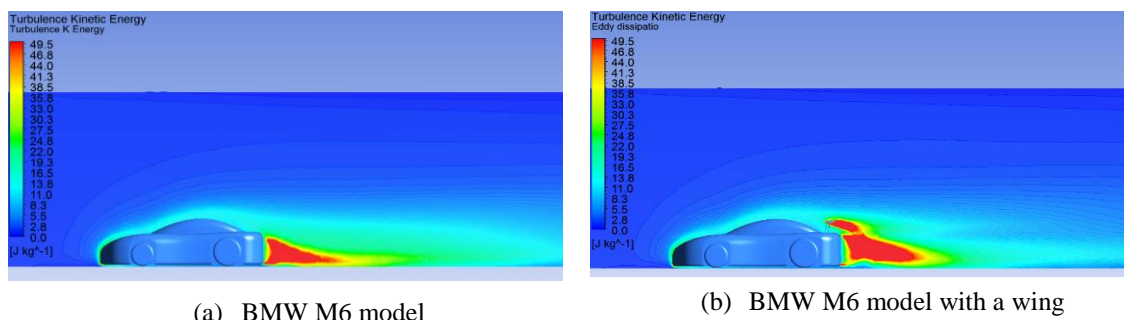
(b) BMW M6 model with a wing

Figure 8. Contours of turbulence kinetic energy distribution around BMW M6 model without/with a wing

Figure 9 illustrates the contours of turbulence eddy dissipation (TED) distribution around BMW M6 model without a wing (Fig. 9a) and with a wing (Fig. 9b). Simulation result indicates that turbulence dissipation behind the car in the case with a wing has a stronger magnitude than in the case without a wing. Therefore, turbulence flow intends stronger after going over the car with a rear wing.

Figure 10 shows the instantaneous isosurfaces on the BMW M6 model without a wing (Fig. 10a) and on the BMW M6 with a wing (Fig. 10b). It is clear to see that the model with a wing has smoothness on the car body's surface, especially on the top surface of the car. The turbulent structures in the head of the model without a wing are denser than which in the head of the model with a wing. The vortical structures at the rear body without a wing are stronger than that at the rear body with a wing. These structures are also generated on the wing in the Figure 10b.
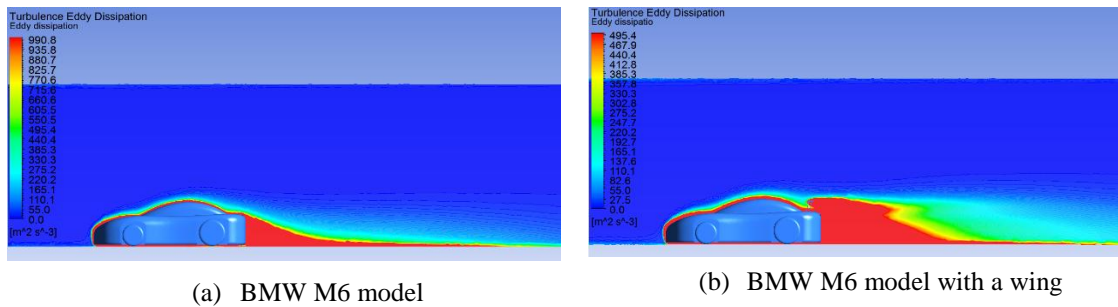
(a) BMW M6 model

(b) BMW M6 model with a wing

Figure 9. Contours of turbulence eddy dissipation distribution around BMW M6 model without/with a wing
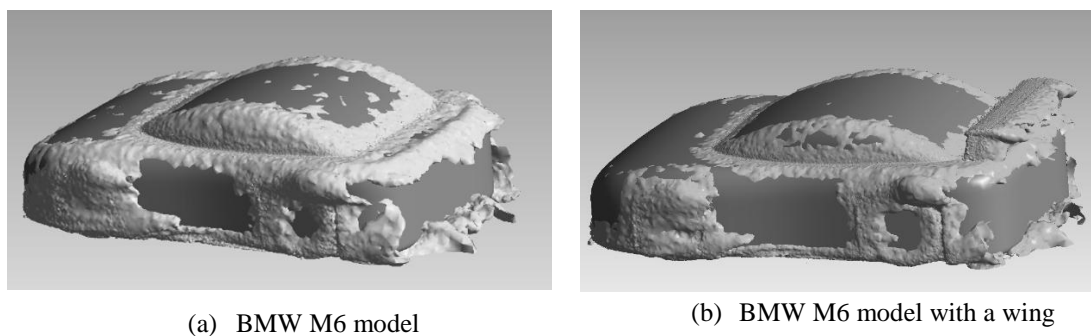

(a) BMW M6 model

(b) BMW M6 model with a wing

Figure 10. Instantaneous isosurfaces on the BMW M6 model without/with a wing

4. CONCLUSIONS

Numerical simulation of air flow over a vehicle is carried out in this study. The air speed is 40 m/s. The 3D Ahmed model with the rear slant angle of 25 degrees is used to validate. In order to estimate effects of a rear wing attached on the vehicle, the BMW M6 model is employed. Results of velocity, pressure, turbulence kinetic energy, turbulence eddy dissipation distributions, streamlines and vortical structures are illustrated and compared with other results. Additionally, calculation results of drag and lift coefficients are shown and compared with many numerical and experimental computations. It found that the rear wing slightly increases the drag coefficient acting on the BMW M6 model and remarkably decreases the lift coefficient acting on the BMW M6 model. Therefore, numerical simulations shown that vehicle can improve its ride stability and cornering performance when a rear wing is attached.

REFERENCES

1. Ahmed S. R., Ramm G., and Faltin G. - Some salient features of the time averagedground vehicle wake, SAE paper no **840300** (1984).

2. Aljure D. E., Lehmkuhl O., Rodríguez I., and Oliva A. - Flow and turbulent structures around simplified car models, Computers & Fluids **96** (2014) 122-135.

3. Brunn A., Wassen E., Sperber D., Nitsche W., and Thiele F. - Active Drag Control for a Generic Car Model, Notes on Numerical Fluid Mechanics and Multidisciplinary Design, DOI: 10.1007/978-3-540-71439-2_15 (2007).

4. Hu X. X., and Wong E. T. T. - A Numerical Study On Rear-spoiler Of Passenger Vehicle, International Journal of Mechanical, Aerospace, Industrial, Mechatronic and Manufacturing Engineering **5** (9) (2011) 1800 – 1805.

5. Kodali S. P., and Bezavada S. - Numerical simulation of air flow over a passenger car and the Influence of rear spoiler using CFD, International Journal of Advanced Transport Phenomena **01** (01) (2012).

6. Meile W., Brenn G., Reppenhagen A., Lechner B., and Fuchs A. -Experiments and numerical simulations on the aerodynamics of the Ahmed body, CFD Letters**3** (1) (2010) 32 – 39.

7. Guilmineau E. -Computational study of flow around a simplified car body, Journal of Wind Engineering and Industrial Aerodynamics **96** (2008) 1207 – 1217.

8. Sagar Kapadia, Subrata Roy, Ken Wurtzler. Detached Eddy Simulation Over a Reference Ahmed Car Model (2003) AIAA-2003-0857.

9. Parab A., Sakarwala A., Paste B., and Patil V. - Aerodynamic Analysis of a Car Model using Fluent- Ansys 14.5, International Journal on Recent Technologies in Mechanical and Electrical Engineering **1** (4) 007-013.

10. Lienhart H., Stoots C., and Becker S. - Flow and Turbulence Structures in the Wake of a Simplified Car Model (Ahmed Model) DOI: 10.1007/978-3-540-45466-3_39 (2002).

11. http://www.sportscarsvs.com